

# Study of GaN Dual-Drain Magnetic Sensor Performance at Elevated Temperatures

Thomas, B., Faramehr, S., Moody, D., Evans, J., Elwin, M. & Igic, P.

Author post-print (accepted) deposited by Coventry University's Repository

## Original citation & hyperlink:

Thomas, B, Faramehr, S, Moody, D, Evans, J, Elwin, M & Igic, P 2019, 'Study of GaN Dual-Drain Magnetic Sensor Performance at Elevated Temperatures', IEEE Transactions on Electron Devices, vol. 66, no. 4, 8663610, pp. 1937 - 1941.  
<https://dx.doi.org/10.1109/TED.2019.2901203>

DOI 10.1109/TED.2019.2901203

ISSN 0018-9383

Publisher: Institute of Electrical and Electronics Engineers (IEEE)

**© 2019 IEEE. Personal use of this material is permitted. Permission from IEEE must be obtained for all other uses, in any current or future media, including reprinting/republishing this material for advertising or promotional purposes, creating new collective works, for resale or redistribution to servers or lists, or reuse of any copyrighted component of this work in other works.**

Copyright © and Moral Rights are retained by the author(s) and/ or other copyright owners. A copy can be downloaded for personal non-commercial research or study, without prior permission or charge. This item cannot be reproduced or quoted extensively from without first obtaining permission in writing from the copyright holder(s). The content must not be changed in any way or sold commercially in any format or medium without the formal permission of the copyright holders.

This document is the author's post-print version, incorporating any revisions agreed during the peer-review process. Some differences between the published version and this version may remain and you are advised to consult the published version if you wish to cite from it.

# Study of GaN Dual-Drain Magnetic Sensor Performance at Elevated Temperatures

B. R. Thomas, S. Faramehr, D. C. Moody, J. E. Evans, M. P. Elwin, and P. Igić

**Abstract**— For the first time, we report on the superior performance of the dual-drain gallium nitride (GaN) magnetic field effect transistor (MagFET) at elevated temperatures. The IV characteristics of the devices reported here were collected under DC conditions and tested at elevated temperatures, 300K, 323K, 373K and 448K using a custom-made heating stage, with a thermal feedback loop to accurately control the temperature. Light exposure experiments were conducted during raised temperature levels using an LED light source of wavelength 470nm. The relative sensitivity of the GaN dual-drain MagFET was calculated and demonstrated a degradation from  $9.78\%T^{-1}$  at 300K, to  $8.36\%T^{-1}$  at 323K,  $6.10\%T^{-1}$  at 373K and  $3.79\%T^{-1}$  at 448K. This is equal to a small sensitivity decrease of  $0.04\%T^{-1}$  per Kelvin. It is proposed that the observed reduction in sensitivity reported herein is due to increased phonon scattering in 2DEG channel. Despite this reduced sensitivity at elevated temperatures, the lowest sensitivity measured at 448K surpasses those reported for silicon competitors.

**Index Terms**— Current Sensor, GaN, MagFETs, Mobility, MOSFET, Scattering, Self-heating.

## I. INTRODUCTION

MAGNETIC field-effect transistors (MagFETs) are MOSFETs modified to detect a magnetic flux by using one source and splitting the drain contact. The double drain MagFETs are ideally suited to current sensing within a standard CMOS process [1]. The integrated MagFET sensors will experience Lorentz force when in the presence of magnetic field strength,  $B$ , that surrounds any current carrying wire within a CMOS circuit. Lorentz force deflects moving charged carriers within the sensor body, thereby creating a current imbalance measurable between the two drains; this imbalance can then be used to calculate the relative sensitivity of the sensor [1], [2]. The use of these integrated MagFETs for current sensing can offer important functions, such as (1) restrict the maximum current supplied, (2) provide a continuous feedback

Submitted for review on 9<sup>th</sup> November 2018. This work was supported by FLEXIS, the European Regional Development Funds (ERDF). We would like to thank industrial collaborators, Compound Semiconductor Centre (CSC) and IQE Europe Limited in Cardiff, Wales for providing us with GaN heterostructures for split-current magnetic sensors fabrication at Swansea University.

B. R. Thomas, D.C. Moody, J. E. Evans and M. P. Elwin are with College of Engineering, Swansea University, Swansea, SA1 8EN, United Kingdom (e-mails: B.R.Thomas@swansea.ac.uk; D.C.Moody@swansea.ac.uk; J.E.Evans@swansea.ac.uk; M.P.Elwin@swansea.ac.uk).

S. Faramehr and P. Igić are with the Institute for Future Transport and Cities, Coventry University, Coventry, CV1 5FB, United Kingdom (e-mails: ad2057@coventry.ac.uk; ad1503@coventry.ac.uk).

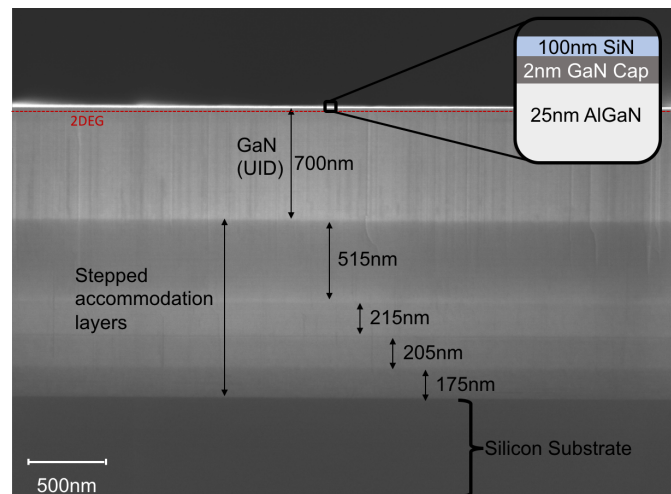


Fig. 1. A cross-sectional scanning electron microscope image of the GaN/Al<sub>0.25</sub>Ga<sub>0.75</sub>N/GaN hetero-structure grown on a silicon substrate with step-graded AlGa<sub>N</sub> accommodation layers. The image shows the measured layers and a diagram magnifying the GaN/AlGa<sub>N</sub> interface with 2DEG (not to scale).

for greater control and (3) detect failures, including a short circuit or open load [3].

However, commercially available MagFETs have material limitations that make them less than ideal for the high power and radio frequency (RF) applications. These limitations include small bandgap value, low thermal conductivity, low carrier mobility and poor channel properties, complicating analysis of systems in real time under high temperatures and/or high radiations [4]. Gallium nitride (GaN) is a better candidate to operate under harsh environments due to several factors including, excellent thermal conductivity, wide bandgap (3.4eV), high electric breakdown field (3.3MV/cm), high electron peak velocity ( $2.5 \times 10^7$ cm/s), high electron saturation velocity ( $1.5 \times 10^7$ cm/s) and its high electron sheet density ( $10^{13}$ cm<sup>-2</sup>) in a readily available heterojunction two-dimensional electron gas (2DEG) channel [5]. The successful heteroepitaxial growth of GaN on a silicon (Si) substrate has also lowered production cost and allowed for the option of integration [4]. For these reasons, the dual-drain GaN magnetic sensor presented here is an ideal candidate for modern power and RF electronics as an integrated additional circuit to sense the current passing through any components and to provide system safety [6].

Nevertheless, self-heating effects within AlGa<sub>N</sub>/GaN high-electron mobility transistors (HEMTs) are still limiting performance parameters, altering device reliability [7]. It follows that it is also of great interest to consider the effect of elevated ambient temperatures, especially considering GaN is marketed as a superior semiconductor material better suited to

function under harsh environmental conditions [5], [6]. This paper reports on temperature controlled electrical measurements for the characterization of the first-ever fabricated GaN dual-drain magnetic high electron mobility transistor (MagHEMT). The results of this study include IV output used to calculate relative sensitivity for the purpose of evaluating the performance of the magnetic sensors held at various elevated temperatures. Later, the results are compared with commercially available sensors in market to show superiority of GaN MagFETs in terms of sensitivity temperature coefficient.

## II. DEVICE AND METHODOLOGY

### A. Fabrication of GaN MagHEMTs

Our fabricated GaN sensors are unintentionally doped GaN/Al<sub>0.25</sub>Ga<sub>0.75</sub>N/GaN heterostructure grown on a silicon substrate with step-graded AlGaN intermediate layers. The GaN cap, AlGaN barrier and GaN buffer thicknesses are 2 nm, 25 nm and 1.8 μm, respectively, refer to Fig. 1 [2]. A 4-inch diameter wafer of GaN on a silicon substrate was diced into smaller 3cm × 3cm wafer pieces and a custom defined 3-mask process was used to fabricate a series of devices onto the small wafers. The first mask enabled the use of an inductively coupled plasma (ICP) system to dry etch the wafers and create mesas, also known as isolated active regions. The second mask was used to pattern Ohmic contacts using plasma vapour deposition (PVD), to sputter deposit a Ti(20nm)/Al(100nm)/Ti(30nm)/Au(100nm) metal stack, followed by a lift-off process and then rapidly annealed at 800°C for a short period of time under N<sub>2</sub> ambient. A standard SiN passivation layer of 100nm was deposited via plasma enhanced chemical vapour deposition (PECVD). Lastly, the third mask allows the removal of passivation from Ohmic contact areas using a fluorine based ICP etch.

The GaN sensor, depicted in Fig. 2 has a source length of  $L_S=5.5 \mu\text{m}$ , drain length of  $L_D=5.5 \mu\text{m}$ , source width of  $W_S=20 \mu\text{m}$ , source to drain distance of  $L_{SD}=24 \mu\text{m}$ . The length and width of fabricated sensors are  $L=35 \mu\text{m}$  and  $W=20 \mu\text{m}$ , respectively and separation between two drain contacts is  $W_{DD}=5 \mu\text{m}$ .

When a positive voltage is applied at D1 and D2, the electric field spreads throughout the 2DEG eventually reaching the

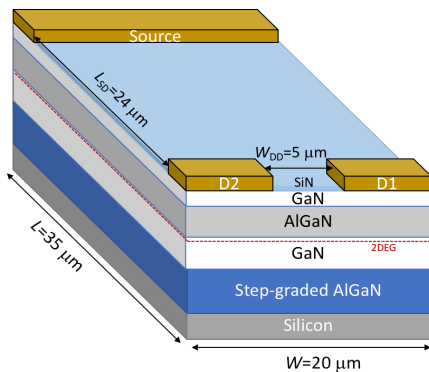


Fig. 2. A 3D diagram (not to scale) of the GaN magnetic sensor.

source, thus allowing for the electric currents,  $I_{DS1}$  and  $I_{DS2}$  to flow between the source and the drains D1 and D2, respectively (Fig. 3). When no magnetic field is present, if the drain contacts have the same effective area, they will receive equal current flow ( $I_{DS1} - I_{DS2} = 0$ ). Current sensors, however, are vulnerable to current offset due to alignment error of sense contacts and inhomogeneities and piezo-resistivity of MagFET material. Therefore, the current offsets are taken into account for sensitivity measurements.

The presence of a magnetic field applied perpendicular to the sensor, causes Lorentz's force to deflect moving charged carriers, leading to a current imbalance calculated by  $|I_{DS1} - I_{DS2}| = |\Delta I| > 0$ . By measuring the  $\Delta I$  one can determine the relative sensitivity ( $S_r$ ), of the sensor by the following equation [8]:

$$S_r = \frac{|I_{DS1} - I_{DS2}|}{I \times |B|} \times 100\% \quad (1)$$

where, relative sensitivity,  $S_r$ , is measured in  $\%T^{-1}$  and  $B$  is the applied magnetic field.

When the total current is much greater than the measured current imbalance the  $S_r$  can be small, however, there are some parameters which can enhance the relative sensitivity.

Relative sensitivity is a function of geometrical parameters and Hall mobility as seen in the following equation [3]:

$$S_r = G\mu_H \frac{L}{W} \quad (2)$$

where,  $G$  is the geometrical correction factor indicating the ratio of electric field distribution in a real Hall plate to ideal Hall plate,  $\mu_H$  is the Hall mobility,  $L$  is the channel length and  $W$  is the device width.

The Hall mobility is also directly affected by Hall scattering, calculated by the following equation [9]:

$$\mu_H = r_H \times \mu \quad (3)$$

where,  $r_H$  is Hall scattering factor and  $\mu$  is effective mobility.

The Hall scattering factor has been shown to increase from 1 to 1.2 in GaN heterostructure as temperature increases from 0 to 300 K [10].

Furthermore, current imbalance is related to the current deflection ( $d$ ) measured in unit length and defined as [11]:

$$d = L\mu_n B \quad (4)$$

where  $L$  is the channel length,  $\mu_n$  is the effective electron mobility.

One may conclude the effect of mobility on the relative sensitivity from equations 2 and 3. At elevated temperatures, scattering rates become larger in an electronic device, thus carrier mobility degrades and consequently the output current reduces [12]–[15].

### B. Temperature Controlled Magnetic Test Unit and Conditions

The magnetic coil shown in Fig. 3 was operated using a separate power supply to increase or decrease voltage, thereby increasing or decreasing the magnetic field produced by the

coil. Also shown in Fig. 3, the iron arms directing the magnetic field perpendicular to the sensors bonded to a PCB carrier board. The motherboard connects the device under-test to a Keithley 4200-SCS semiconductor characterization system with 200V/1A DC, with pulse and CV measurement capability. During all tests source contacts were kept at 0 V and a 0.5 V bias was applied to Drain 1 (D1) and Drain 2 (D2) for 15 seconds before current measurements were logged. During these 15 seconds the voltage of the coil was increased manually. The magnetic coil power supply was varied from 0 V to 3.6 V in steps of 0.2 V, to achieve a magnetic range of 0.7 mT to 31.4 mT. The sensors were tested at four different temperatures 300K, 323K, 373K and 448K using the heated copper stage. The heated stage was given adequate time for the temperature to stabilize before any tests were conducted, this was determined by a continuously held temperature displayed on the control panel. The entire heating unit is situated inside of a metal box with closing lid. The sensors were allowed 600 seconds of rest in darkness before testing, this avoids any variation in current due to ambient lighting conditions [16].

### III. EXPERIMENTAL RESULTS AND DISCUSSION

Fig. 4 (a) shows that during 100 seconds of exposure to an external light source, the current increases for all three devices with  $\text{Si}_3\text{N}_4$  passivation thicknesses, 5nm, 50nm and 100nm. The current decreases again when the external source is removed. The initial current measured for 5nm passivation during 100 seconds of darkness is the lowest of all three samples but demonstrates the greatest increase under light exposure. A higher initial current was measured for 50nm passivation in the first 100 seconds of darkness and a smaller increase in current during exposure to external light. The 100nm passivation recorded the highest initial current during the first 100 seconds of darkness and had a similar increase in current to 50nm when exposed to external light. The increase in current under illumination recorded in all samples is due to the excitation of surface states by photons which generate more carriers, thereby contributing to the current. The recombination of photogenerated carriers post light exposure causes the current to return to its lower level [17]. Fig. 4 (a) demonstrates that a thicker  $\text{Si}_3\text{N}_4$  passivation layer maintains a greater output current; it is reported that passivation reduces the formation of

surface states and causes an increase in carriers in the 2DEG [18]. The output current increases from 15.55mA at 5nm to 15.9mA at 100nm passivation due to lowering of trap ionization energy [19] and steady state condition is reached earlier for 100nm passivation once light perturbation is removed. At 5nm passivation polarization charge is partially compensated, therefore, it is more prone to light exposure and a larger current peak is observed when exposed to light. Recent studies have reported that these surface state distribution may emerge during deposition of the passivation layer [20]. Since dielectric traps capture cross section are not scalable, further improvement in surface morphology to enhance uniformity and quality of dielectric film deposition would help with device stability and reliability [21].

Fig. 4 (b) illustrates how the current imbalance divided by the total current measured at D1 and D2 is reduced at elevated temperatures and also demonstrates how light exposure can further reduce this ratio. As previously seen in Fig. 4 (a), the photons produced by the light source generated higher currents in the GaN sensor, which has resulted in a greater total current measured at D1 and D2 compared to the imbalance.

Since sensitivity is dictated by the ratio of current imbalance to total current, refer to (1), as the ratio is decreased the sensitivity of the GaN sensors is also reduced. Due to effects of light exposure on the sensors, all further tests reported herein

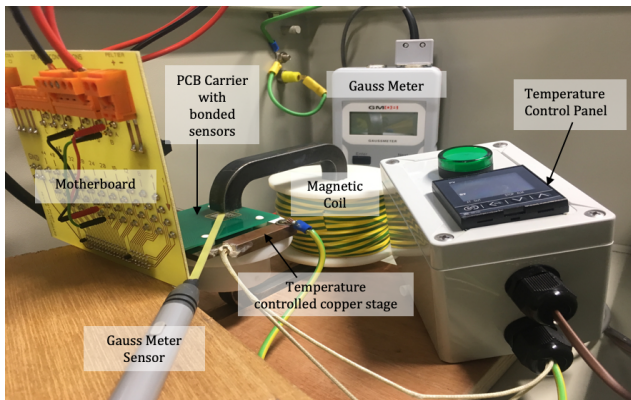


Fig. 3. A labelled picture the custom-built heating unit used to test the sensors. The heating unit is stationed inside a large blackout box allowing for complete darkness during experiments and avoiding variations due to light exposure.

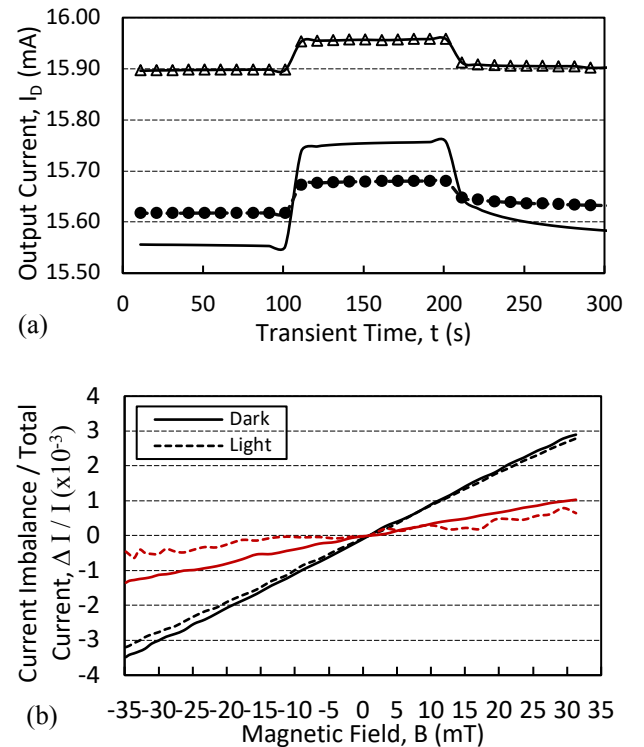


Fig. 4. (a) Transient current measured at 300K over a total of 300 seconds held at  $V_{DS} = 0.5$  V, broken down into 100 seconds in darkness, 100 seconds under LED white light source ( $\lambda = 470$ nm) and a further 100 seconds in darkness. Sensors tested were fabricated identically except for different  $\text{Si}_3\text{N}_4$  passivation thicknesses, 5 nm, 50 nm and 100 nm. All sensors were allowed an initial 10 minutes rest in darkness. Fig. 4. (b) Ratio of current imbalance to total current measured during increasing magnetic field strength ( $B = -34.8$  mT to  $B = 31.4$  mT), held at  $V_{DS} = 0.5$  V. Current measured at 300K (Black), and 448K (Red) collected under dark (solid line) and light (dash line) conditions (LED white source,  $\lambda = 470$ nm).

were conducted under dark conditions in order to reduce variability that may be caused by changing environmental light and to optimize sensitivity measurements.

Fig. 5 shows IV measurements repeated 3 times at elevated temperatures 300K, 323K, 373K and 448K. The graph displays voltage saturation effects at the higher bias. Also observed in the graph, is decreasing current with increasing temperature, from 300K to 448K, this is likely due to increased scattering mechanisms within the sensor, thereby degrading mobility [14], [15]. There are several sources of scattering in GaN HEMTs, interface roughness between the AlGaIn top layer and the 2DEG channel, dislocation scatterings [22], ionized impurity scattering [23] and phonon scattering [7]. Ionized impurity

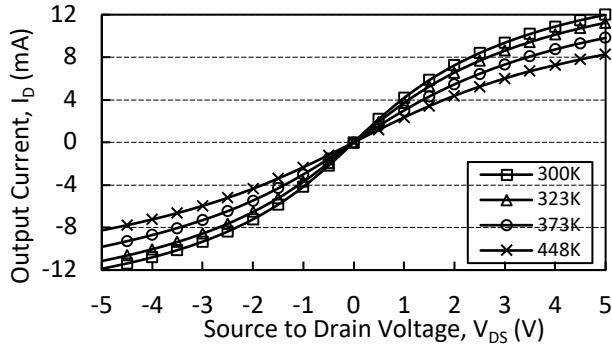


Fig. 5. Sensor current against drain-source voltage sweeping from -5 V to 5 V, in steps of 0.5 V. The current was measured at 300K, 323K, 373K and 448K.

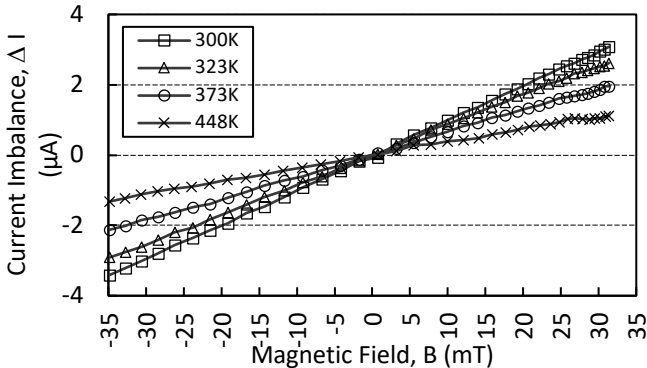


Fig. 6. Current imbalance obtained from fabricated sensor held at  $V_{DS} = 0.5$  V against increasing magnetic field strength ( $B = -34.8$  mT to  $B = 31.4$  mT) measured at 300K (Squares), 323K (Triangles), 373K (Circles), and 448K (Crosses).

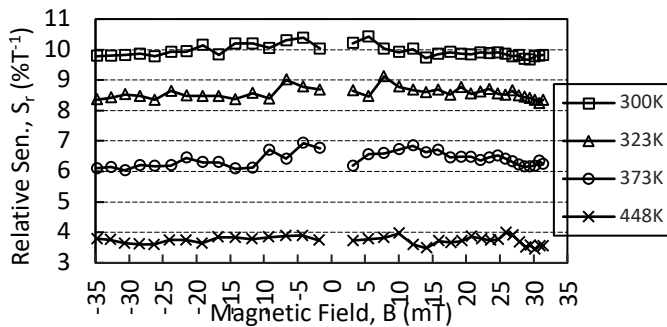


Fig. 7. Relative sensitivity obtained from fabricated sensor held at  $V_{DS} = 0.5$  V against increasing magnetic field strength ( $B = -34.8$  mT to  $B = 31.4$  mT) measured at 300K (Squares), 323K (Triangles), 373K (Circles), and 448K (Crosses).

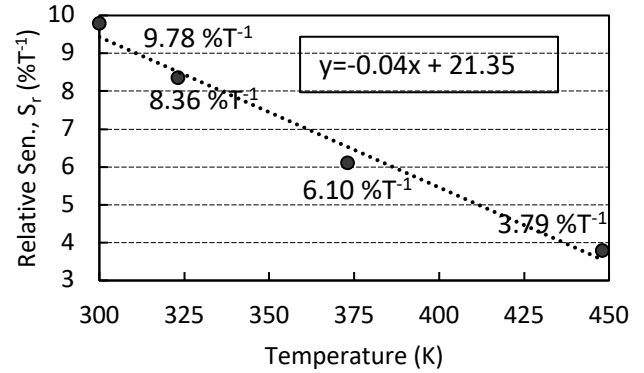


Fig. 8. Relative sensitivity of sensor as a function of temperature in Kelvin.

scattering has been shown to effect mobility at low temperatures, but phonon scattering becomes the dominant source of scattering as temperatures increases above 300K. Additionally, surface roughness can contribute at high and low temperature [7], [14], [15]. As all temperatures tested in this study were above 300K, phonon scattering is considered to be cause of the decreasing current observed, with some contribution from surface roughness [7], [10], [24].

Fig. 6 shows that at all temperatures increasing magnetic field strength increases the current imbalance measured between D1 and D2 contacts but the total current and the calculated imbalance falls with each temperature rise.

The relative sensitivity calculated using (1) is depicted in Fig. 7, revealing that increasing temperatures decrease the sensitivity of the sensors. At the highest magnetic field strength 31.4mT, the relative sensitivity equalled 9.78%T<sup>-1</sup> at 300K, to 8.36% at 323K, 6.10%T<sup>-1</sup> at 373K and 3.79%T<sup>-1</sup> at 448K (see Fig. 8).

Equation (2), (3) and (4) dictate that relative sensitivity is a function of geometrical parameters, i.e. the geometrical correction factor ( $G$ ), Hall mobility ( $\mu_H$ ), Hall scattering factor ( $r_H$ ), electron mobility ( $\mu_n$ ), device channel length ( $L$ ) and width ( $W$ ). Since no geometrical parameters were varied and fabricated and tested under the same conditions, the decrease in relative sensitivity observed at elevated temperatures is assigned to mobility degradation of the electrons in 2DEG channel as a result of increased phonon scattering [7], [14], [15].

Compared to a silicon dual-drain current sensor reported by R. Rodriguez-Torres et al (2004) with the optimized geometry and relative sensitivity of 3.64% T<sup>-1</sup> at 300 K, the GaN current sensor reported here shows a superior performance at elevated temperatures with measured relative sensitivity of 3.79 %T<sup>-1</sup> at 448 K.

The majority of commercially available sensors including automotive current transducers have operating temperatures ranging between -40 °C to 125 °C. To the best of authors' knowledge, there is no current transducer capable of operating at 175 °C (448K) and above without temperature compensation element to account for sensitivity drift and output signal amplifier to recover the weak output signal.

The GaN current sensors herein were measured at elevated temperatures without additional circuitries at terminals to strengthen the output signal or to account for temperature compensation. Therefore, they are capable of operating at

temperatures above of currently reported, 448K, using more advanced thermal unit utilized for this study and supporting circuitries.

While operating the Hall-effect device from a constant voltage bias source, one will find sensitivity variation to be considerably greater than of those obtained by constant current source. Therefore, large sensitivity value of the current sensors is of an importance for device operating at elevated temperatures with a constant voltage source.

Since output of Hall-effect devices is a function of operating temperature, the sensitivity change needs to be accounted and corrected when a high degree of stability is needed in some applications. One method to improve the temperature stability is the temperature compensation, an amplifier with a temperature dependent gain.

#### IV. CONCLUSION

We studied the GaN current sensors performance and relative sensitivity at elevated temperatures (300K to 448K), attributed to increased phonon scattering, hence lowering both mobility and saturation velocity [12]–[15]. Although the GaN sensors reported show decreasing current output and sensitivity at elevated temperatures, when compared to other competitors including silicon Hall-effect devices the values reported here are very promising. At 448K we recorded  $3.79\%T^{-1}$ , which is greater than sensitivities reported for optimised silicon dual-drain current sensors at 300K [25], [26]. These findings demonstrate the great potential of the GaN MagHEMTs as a superior current sensor when required to function at higher temperatures.

#### REFERENCES

- [1] J. W. A. Von Kluge and W. A. Langheinrich, "An analytical model of MAGFET sensitivity including secondary effects using a continuous description of the geometric correction factor G," *IEEE Trans. Electron Devices*, vol. 46, no. 1, pp. 89–95, 1999.
- [2] R. Rodríguez-Torres, E. A. Gutiérrez-Domínguez, R. Klima, and S. Selberherr, "Analysis of split-drain MAGFETs," *IEEE Trans. Electron Devices*, vol. 51, no. 12, pp. 2237–2245, Dec. 2004.
- [3] F. C. Castaldo, V. R. Mognon, and C. A. dos Reis Filho, "Magnetically Coupled Current Sensors Using CMOS Split-Drain Transistors," *IEEE Trans. Power Electron.*, vol. 24, no. 7, pp. 1733–1736, Jul. 2009.
- [4] Shih-Hung Chen *et al.*, "HBM ESD Robustness of GaN-on-Si Schottky Diodes," *IEEE Trans. Device Mater. Reliab.*, vol. 12, no. 4, pp. 589–598, Dec. 2012.
- [5] B. Shankar and M. Shrivastava, "Unique ESD behavior and failure modes of AlGaIn/GaN HEMTs," in *2016 IEEE International Reliability Physics Symposium (IRPS)*, 2016.
- [6] P. Igetic, N. Jankovic, J. Evans, M. Elwin, S. Batcup, and S. Faramehr, "Dual-Drain GaN Magnetic Sensor Compatible with GaN RF Power Technology," *IEEE Electron Device Lett.*, p. 1, 2018.
- [7] E. Pichonat *et al.*, "Temperature analysis of AlGaIn/GaN high-electron-mobility transistors using micro-Raman scattering spectroscopy and transient interferometric mapping," in *Proceedings of the 1st European Microwave Integrated Circuits Conference, EuMIC 2006*, 2007.
- [8] N. Jankovic, O. Kryuchenkova, S. Batcup, and P. Igetic, "High sensitivity dual-gate four-terminal magnetic sensor compatible with SOI Fin FET technology," *IEEE Electron Device Lett.*, vol. 38, no. 6, pp. 810–813, Jun. 2017.
- [9] G. Ng, D. Vasileska, and D. K. Schroder, "Calculation of the electron Hall mobility and Hall scattering factor in 6H-SiC," *J. Appl. Phys.*, vol. 106, no. 5, p. 53719, Sep. 2009.
- [10] A. Asgari, S. Babanejad, and L. Faraone, "Electron mobility, Hall scattering factor, and sheet conductivity in AlGaIn/AlN/GaN heterostructures," *J. Appl. Phys.*, vol. 110, no. 11, p. 113713, Dec. 2011.
- [11] R. Rodríguez-Torres, R. Klima, S. Selberherr, and E. A. Gutiérrez-D., "Three-dimensional analysis of a MAGFET at 300K and 77K," in *European Solid-State Device Research Conference*, 2002.
- [12] N. Maeda, K. Tsubaki, T. Saitoh, and N. Kobayashi, "High-temperature electron transport properties in AlGaIn/GaN heterostructures," *Appl. Phys. Lett.*, vol. 79, no. 11, pp. 1634–1636, Sep. 2001.
- [13] O. Aktas, Z. F. Fan, S. N. Mohammad, A. E. Botchkarev, and H. Morkoç, "High temperature characteristics of AlGaIn/GaN modulation doped field-effect transistors," *Appl. Phys. Lett.*, vol. 69, no. 25, p. 3872, Jun. 1998.
- [14] M. S. Pramanick and A. Ghosal, "Effects of scattering on transport properties in GaN," in *Proceedings of 2nd International Conference on 2017 Devices for Integrated Circuit, DevIC 2017*, 2017.
- [15] M. N. Gurusinge, S. K. Davidsson, and T. G. Andersson, "Two-dimensional electron mobility limitation mechanisms in Al<sub>x</sub>Ga<sub>1-x</sub>N/GaN heterostructures," *Phys. Rev. B - Condens. Matter Mater. Phys.*, vol. 72, no. 4, p. 045316, Jul. 2005.
- [16] S. Arulkumaran, T. Hibino, T. Egawa, and H. Ishikawa, "Current collapse-free i-GaN/AlGaIn/GaN high-electron-mobility transistors with and without surface passivation," *Appl. Phys. Lett.*, vol. 85, no. 23, pp. 5745–5747, Dec. 2004.
- [17] M. Reshchikov, P. Visconti, K. Jones, H. Morkoc, R. Molnar, and C. Litton, "Recombination at surface states in GaN," in *Materials Research Society Symposium Proceedings*, 2001.
- [18] R. Vetry, N. Q. Zhang, S. Keller, and U. K. Mishra, "The impact of surface states on the DC and RF characteristics of AlGaIn/GaN HFETs," *IEEE Trans. Electron Devices*, vol. 48, no. 3, pp. 560–566, Mar. 2001.
- [19] Hyungtak Kim, R. M. Thompson, V. Tilak, T. R. Prunty, J. R. Shealy, and L. F. Eastman, "Effects of SiN passivation and high-electric field on AlGaIn-GaN HFET degradation," *IEEE Electron Device Lett.*, vol. 24, no. 7, pp. 421–423, Jul. 2003.
- [20] N. Goyal and T. A. Fjeldly, "Surface donor states distribution post SiN passivation of AlGaIn/GaN heterostructures," *Appl. Phys. Lett.*, vol. 105, no. 3, p. 33511, Jul. 2014.
- [21] H. Wong and V. A. Gritsenko, "Defects in silicon oxynitride gate dielectric films," *Microelectron. Reliab.*, vol. 42, no. 4–5, pp. 597–605, Apr. 2002.
- [22] S. W. Kaun, P. G. Burke, M. Hoi Wong, E. C. H. Kyle, U. K. Mishra, and J. S. Speck, "Effect of dislocations on electron mobility in AlGaIn/GaN and AlGaIn/AlN/GaN heterostructures," *Appl. Phys. Lett.*, vol. 101, no. 26, p. 262102, Dec. 2012.
- [23] F. Schubert, S. Wirth, F. Zimmermann, J. Heitmann, T. Mikolajick, and S. Schmult, "Growth condition dependence of unintentional oxygen incorporation in epitaxial GaN," *Sci. Technol. Adv. Mater.*, vol. 17, no. 1, pp. 239–243, 2016.
- [24] D. Zanato, S. Gokden, N. Balkan, B. K. Ridley, and W. J. Schaff, "The effect of interface-roughness and dislocation scattering on low temperature mobility of 2D electron gas in GaN/AlGaIn," *Semicond. Sci. Technol.*, vol. 19, no. 3, pp. 427–432, Mar. 2004.
- [25] M. Daříček, M. Donoval, and A. Šatka, "Behavior of various geometry MagFET structures," in *ECCTD 2009 - European Conference on Circuit Theory and Design Conference Program*, 2009.
- [26] N. Rezaei, R. Dehghani, A. Jalili, and A. Mosahebfard, "CMOS magnetic sensor with MAGFET," in *2013 21st Iranian Conference on Electrical Engineering, ICEE 2013*, 2013.